



Title	Particle-in-cell simulation on the mechanism and scalability of Terahertz Generation from atmosphere plasma ionized by two-color fs laser
Author(s)	Junghun, Shin; Alexei, Zhidkov; Zhan, Jin et al.
Citation	サイバーメディアHPCジャーナル. 2013, 3, p. 11-15
Version Type	VoR
URL	https://doi.org/10.18910/70465
rights	
Note	

The University of Osaka Institutional Knowledge Archive : OUKA

<https://ir.library.osaka-u.ac.jp/>

The University of Osaka

Particle-in-cell simulation on the mechanism and scalability of Terahertz Generation from atmosphere plasma ionized by two-color fs laser

Junghun Shin¹⁾, Alexei Zhidkov²⁾, Zhan Jin²⁾, Tomonao Hosokai²⁾, Ryosuke Kodama^{1,2,3)}

¹⁾*Graduate School of Engineering, Osaka University*

²⁾*Photon Pioneers Center, Osaka University*

³⁾*Institute of Laser Engineering, Osaka University*

Introduction

Recent years have seen a growing interest in nonlinear interactions between intense THz electromagnetic fields and materials including warm dense matters, semiconductors, nanostructure materials [1–4]. Generation of intense THz electromagnetic field whose electric field is stronger than 1 MV/cm is critical to pave the way for new studies and applications in this direction. One of the promising approaches is to use plasma as the radiation source. Plasma by its nature does not have damage threshold in contrast to other conventional methods using solid nonlinear crystals [5]. It has been demonstrated that a nonrelativistic laser can efficiently generate THz radiation, given that the laser has two frequency components, namely, a fundamental frequency ω and its second harmonic 2ω [6–9].

One obvious way to increase the THz power with this two-color laser scheme is to increase the incident laser power. However, as the laser intensity increases, nonlinear plasma effects become essential and may negatively result in THz radiation. Despite of numerous experimental works on the topic, there is a clear lack of theoretical and numerical examination of THz radiation during the interaction of realistic femtosecond laser pulses with underdense plasma.

This reflects the numerosity of physical processes that result in THz radiation during the laser pulse irradiation and afterward: the processes of frequency up-shift in the front of a pulse and k vector downshift

in the rear resulting in beat waves; pulse modulation owing to the refraction on the electron density ramp; steep plasma boundary, etc. All instabilities inherent to plasma result in THz radiation in a certain range of wavelengths and in a direction determined by a process of radiation; dispersion effects in plasma on THz radiation occurring at higher density plasma have yet to be understood. Due to the nonlinear nature of those phenomena, it is hardly possible to carry out an analytical examination incorporating all the nonlinear processes involved in the THz radiation emission from strongly ionized air.

It is therefore necessary to look into the interaction between femtosecond laser pulses and underdense plasma with kinetic simulations that self-consistently include plasma and atomic physics [10–13].

In the report, a numerical study on the mechanism and scaling law of THz generation with a co-propagating two-color laser pulse in air is presented for the peak fundamental laser intensities of 10^{14} , 10^{15} and 10^{16} W/cm².

Description of Particle Calculation Method

To take into account the most important effects, the particle-in-cell simulation including ionization kinetics has to be performed. In this work, the variable particle weight method is used to calculate the particle density, which is based on the solution of balance equations for density and energy [14]:

$$dN_i / dt = S_{i-1}N_{i-1} - (S_i + R_i)N_i + R_{i+1}N_{i+1},$$

$$N_e = \sum_{i=1} iN_i, N_D = \sum_{i=0} N_i, dE / dt = 0 \quad (1)$$

where S_i, R_i are the total ionization and recombination rates for i^{th} ion, N_e is the electron density, N_D is the gas density, E is the total energy. The charge growth is calculated as $\Delta Q_M = \pm e\Delta t V_M \sum_{k=0} S_k N_k$ and is

redistributed over all particles in a kinetic cell M with its volume V_M with the correction of their kinetic energy.

In case of optical field by femtosecond laser pulses and within a relatively short time of simulation, recombination can be ignored and the ionization equations in Eq. (1) can be simplified as $dN_i / dt = S_{i-1}N_{i-1}$. The ionization rate is written in the well known approximation [6-9]:

$$S_k = 4\omega_A g_k \left(\frac{I_k}{Ry} \right)^{5/2} \frac{E_A}{E} \exp \left(-\frac{2}{3} \left(\frac{I_k}{Ry} \right)^{3/2} \frac{E_A}{E} \right) \quad ,$$

where $\omega_A = me^4 / \hbar^3$ and $E_A = m^2 e^5 / \hbar^4$ the atomic frequency and atomic electric field strength; $Ry = m^2 e^4 / 2\hbar^2$, I_k is the potential for ion with charge k ; g_k is a factor ~ 1 , E is an external field strength. The energy conservation is achieved by introducing an atomic current, which provides the Ohmic heating equivalent to the power loss for the ionization:

$$\vec{j}_A E^2 = \sum_{k=0} I_k S_k N_k, \text{ to Maxwell equations.}$$

Results and Discussion

To study the characteristics of THz radiation, PIC simulations using FPLaser2D [13] with a moving window were performed for a linearly polarized laser pulse propagating in air under normal pressure. The 2D

calculations are performed for the laser intensity from 10^{14} (which is about the threshold intensity for air) to 10^{16} W/cm^2 and 90 fs FWHM duration. The calculations are performed for a two-color laser pulse whose wavelength consists of $\lambda = 0.8 \mu\text{m}$ and $\lambda_1 = 0.4 \mu\text{m}$. Both are p-polarized. The total energy in the second harmonic is ~ 0.3 times the energy of

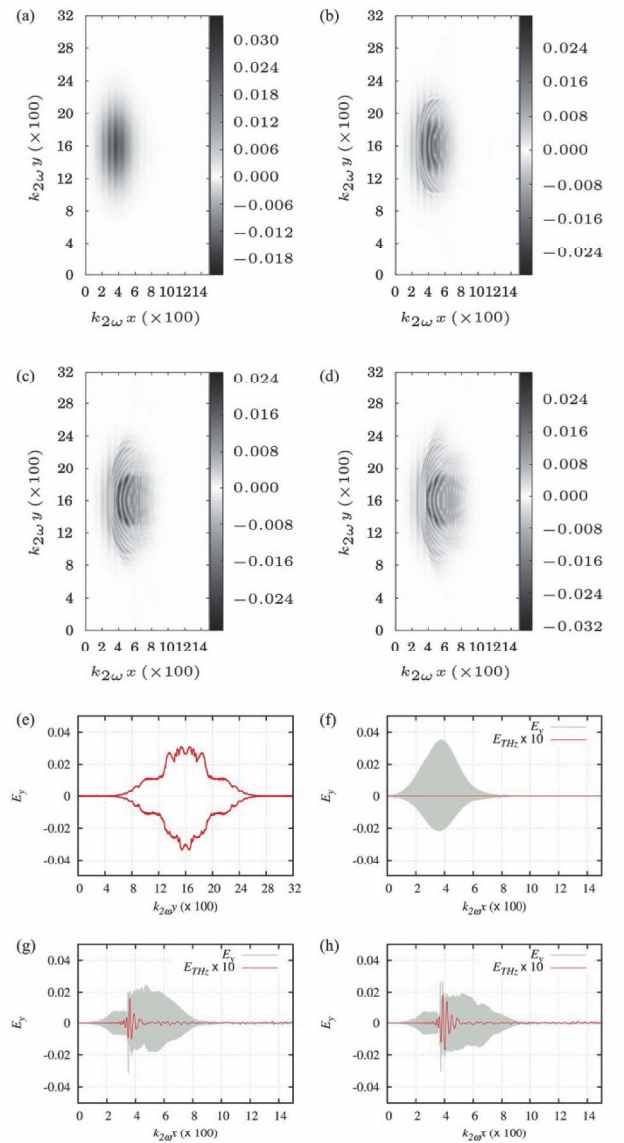


Fig. 1. (a-d) *p*-polarized electric fields over simulation area after 0.1, 2.1, 3.6 and 4.2 ps after propagation in the gas, (e) transverse profile at 4.2 ps, and (f-h) profile along laser propagation axis x corresponding to (a), (c) and (d), respectively. The peak intensity of fundamental pulse is $I_\omega = 10^{16} \text{ W/cm}^2$, and 2ω at $I_{2\omega} = 0.3 I_\omega$.

fundamental harmonic. The focus spot of the fundamental harmonic is chosen to provide the Rayleigh length on the order of 1 mm; the focus spot of the second harmonic is same as that of fundamental harmonic. The size of the simulation window is 320 μm by 150 μm and $\lambda_l/10$ spatial resolution; the kinetic cell is twice as large as the PIC one. The kinetic simulation was simplified by including only nitrogen molecules; the laser pulse is set as Gaussian.

Fig. 1 shows the time evolution of the electric field of the p -polarized two-color laser pulse propagating in the air. The intensity of the fundamental pulse is $I = 10^{16} \text{ W/cm}^2$ at the focus point. **Fig. 3** shows the particle densities for electrons and ions under the same simulation condition. The maximal electron density in

this case is $N_e^{\max} = 3 \times 10^{19} \text{ cm}^{-3}$. Therefore, plasma is almost fully ionized. The maximal plasma frequency is about $\omega_{\text{pl}} \sim \omega/8$ or $\nu \sim 40 \text{ THz}$. One can see modulations of the laser field strength both in longitudinal and transverse directions. The refraction of laser field by results in the density decrease and, consequently weaker, but further refraction according to the eikonal equation:

$$d\theta / dx = -0.5 \nabla_{\perp} [N_e(\theta) / N_{cr}]$$

, where θ is the angle of light beam propagation. This process is nonlinear as seen in **Fig. 1e**. The modulation of the central part of the laser pulse owes the refraction effect while the modulation of pulse wings is the THz radiation. The most powerful part of the THz radiation can be seen in **Fig. 1h** in the middle of the field. The

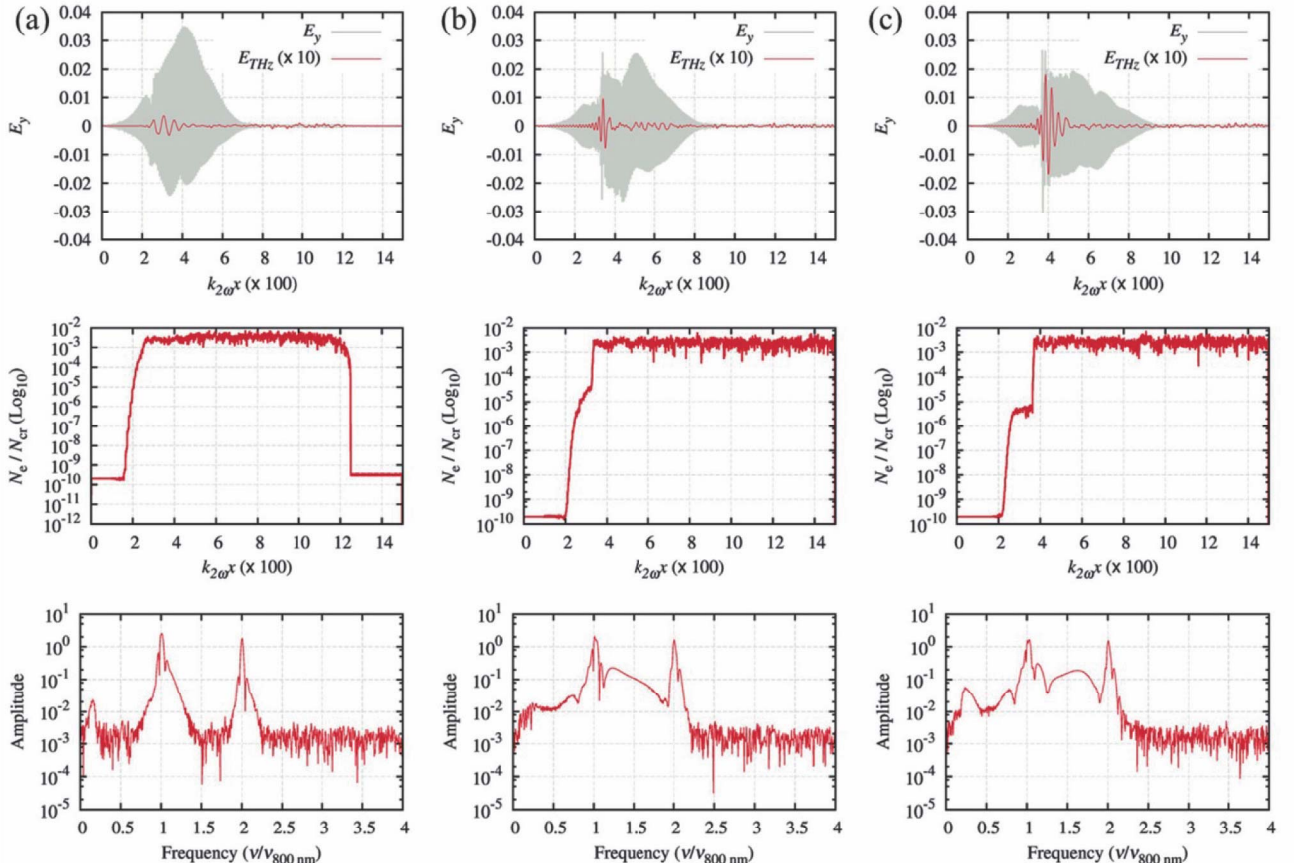


Fig. 2. Temporal evolution of the laser field and THz radiation along with the plasma density and spectra with a laser pulse which comprises of both fundamental and second harmonic components. The peak intensity of fundamental pulse is 10^{16} W/cm^2 . From (a) to (c), they are taken at $t=0.1, 2.1$ and 4.2 ps after laser propagation in the gas.

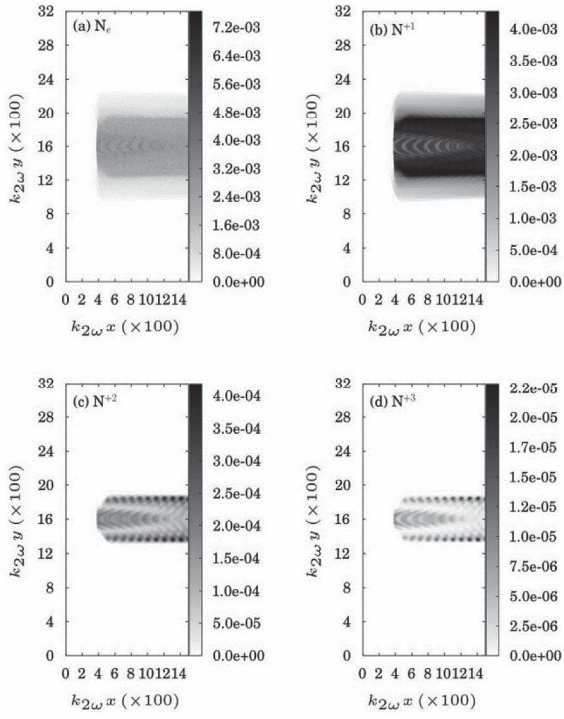


Fig. 3. Electron and ion densities after propagation of a *p*-polarized two-color laser pulse in air with the peak intensity of ω at $I_\omega = 10^{16}$ W/cm² and 2ω at $I_{2\omega} = 0.3 I_\omega$. (a) electron density, (b-d) density of 1+, 2+ and 3+ nitrogen ion, respectively.

Duration of THz impulse is about 7 fs which displays a broad spectrum of that long wavelength radiation. That agrees well with previous theoretical work [15]. THz pulse cuts the laser pulse into two parts: the front part initially responsible for the optical ionization is essentially depleted while the second, rear part has almost intact Gaussian profile.

To reveal the process of THz radiation formation, the temporal evolution of the laser field and THz radiation along with the plasma density and spectra is shown in. **Fig. 3.** The THz radiation is calculated as inverse Fourier transformation with short wavelengths cut-off. One can see that THz radiation occur initially a little bit far from the ionization front. Then the strong steeping of electron density is observed along with the THz power increase. Therefore, the long wavelength

radiation can propagate straightforward. Corresponding spectra exhibit the strong up-shift frequency components for both the fundamental and second harmonics and the correlation between the frequency up-shift and the frequency of THz radiation. It reveals one of the main mechanisms of formation of THz radiation; the ionization current creates beat waves whose characteristics depend on the ionization frequency up-shift. Interference of the beat wave with the second harmonics radiation is the sources of the current oscillating at the frequency of $2\omega_p$ which is responsible for the long wavelength radiation.

We also performed the calculation of two-color *p*-polarized pulses with lower intensities. The dependence of power of THz radiation on the laser pulse intensity is presented in **Fig. 4** in which the THz power generated by different laser intensities are shown for two THz propagation angle, namely, 0 and 30 degrees. In both cases one can see two different slopes in the curves: up to the laser intensity $I \sim 10^{15}$ W/cm², the power growth is faster than linear, while after the growth is slower than linear. An approximation function can be presented as following: $W \approx A(I/B)^\alpha e^{-B/I}$ with $\alpha = 0.7$, $A = 9 \times 10^{-3}$, and $B = (2 - 3) \times 10^{14}$ W/cm².

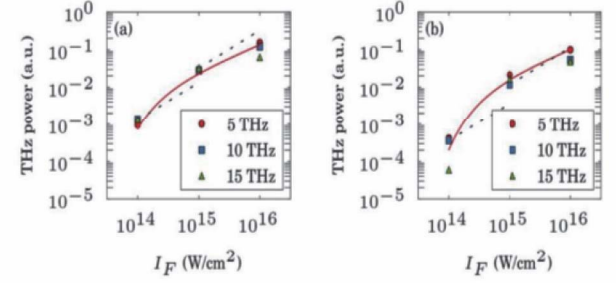


Fig. 4. The dependence of power of THz radiation on the laser pulse intensity at the emission angles at (a) 0° and (b) 30°. Dotted lines indicates linear growth of THz power against the laser intensity.

Conclusion

In conclusion, a numerical study on the mechanism and dependence of THz power radiated from air plasma produced by femtosecond laser pulse with fundamental and second harmonic components is presented. Beat wave generation between waves with and without frequency shift induced by laser-produced plasma is observed and attributed to the formation mechanism of the THz radiation. On the scalability of THz radiation by the two-color laser scheme, we have found strong non-linear dependence of the THz power on the laser intensity. The power growth is faster than linear up to laser intensities on the order of $I \sim 10^{15}$ W/cm², then, the growth becomes slower than the linear; therefore our results show that the conversion efficiency reaches its maximum at $I \sim 10^{15}$ W/cm².

Acknowledgements

Author is grateful for the support of the computer room of ILE and the Cybermedia Center at Osaka University. This study was supported by Japan Science and Technology CREST and Global COE program in Ministry of Education, Culture, Sports, Science and Technology (Electronic Devices Innovation).

References

- [1] B. E. Cole, J. B. Williams, B. T. King, M. S. Sherwin, and C. R. Stanley, *Nature* **410**, 60 (2001).
- [2] T. Kampfrath, L. Perfetti, F. Schapper, C. Frischkorn, and M. Wolf, *Physical Review Letters* **95**, 187403 (2005).
- [3] P. Gaal, K. Reimann, M. Woerner, T. Elsaesser, R. Hey, and K. Ploog, *Physical Review Letters* **96**, 187402 (2006).
- [4] C. Kübler, H. Ehrke, R. Huber, R. Lopez, A. Halabica, R. Haglund, and A. Leitenstorfer, *Physical Review Letters* **99**, 116401 (2007).
- [5] X.-C. Zhang, Y. Jin, and X. F. Ma, *Applied Physics Letters* **61**, 2764 (1992).
- [6] D. J. Cook and R. M. Hochstrasser, *Optics Letters* **25**, 1210 (2000).
- [7] T. Bartel, P. Gaal, K. Reimann, M. Woerner, and T. Elsaesser, *Optics Letters* **30**, 2805 (2005).
- [8] X. Xie, J. Dai, and X.-C. Zhang, *Physical Review Letters* **96**, 075005 (2006).
- [9] K. Y. Kim, A. J. Taylor, J. H. Gownia, and G. Rodriguez, *Nature Photonics* **2**, 605 (2008).
- [10] M. Chen, A. Pukhov, X.-Y. Peng, and O. Willi, *Physical Review E* **78**, 046406 (2008).
- [11] H.-C. Wu, J. Meyer-ter-Vehn, and Z.-M. Sheng, *New Journal of Physics* **10**, 043001 (2008).
- [12] N. A. Zharova, V. A. Mironov, and D. A. Fadeev, *Physical Review E* **82**, 056409 (2010).
- [13] A. Zhidkov, T. Esirkepov, T. Fujii, K. Nemoto, J. Koga, and S. V. Bulanov, *Physical Review Letters* **103**, 215003 (2009).
- [14] A. Zhidkov and A. Sasaki, *Physics of Plasmas* **7**, 1341 (2000).
- [15] I. Babushkin, W. Kuehn, C. Köhler, S. Skupin, L. Bergé, K. Reimann, M. Woerner, J. Herrmann, and T. Elsaesser, *Physical Review Letters* **105**, 053903 (2010).